J. Fluid Mech. (1998), *vol.* 366, *pp.* 135–158. Printed in the United Kingdom

Stability of hydromagnetic dissipative Couette flow with non-axisymmetric disturbance

By CHA'O-KUANG CHEN AND MIN HSING CHANG
Department of Mechanical Engineering, National Cheng Kung University, Tainan, Taiwan 701

(Received 12 September 1996 and in revised form 27 January 1998)

A linear stability analysis has been implemented for hydromagnetic dissipative Couette flow, a viscous electrically conducting fluid between rotating concentric cylinders in the presence of a uniform axial magnetic field. The small-gap equations with respect to non-axisymmetric disturbances are derived and solved by a direct numerical procedure. Both types of boundary conditions, conducting and non-conducting walls, are considered. A parametric study covering wide ranges of μ, the ratio of angular velocity of the outer cylinder to that of inner cylinder, and Q, the Hartmann number which represents the strength of axial magnetic field, is conducted. Results show that the stability characteristics depend on the conductivity of the cylinders. For the case of non-conducting walls, it is found that the critical disturbance is a non-axisymmetric mode as the value of μ is sufficiently negative and the domain of Q where non-axisymmetric instability modes prevail is limited. Similar results are obtained for conducting walls at low Hartmann number. In addition, the transition of the onset of instability from non-axisymmetric modes to axisymmetric modes for the case $\mu = -1$ with increasing strength of magnetic field are discussed in detail. For high values of the Hartmann number, the critical disturbance is always the axisymmetric stationary mode for non-conducting walls but not for conducting walls. For $-1 \leqslant \mu < 1$, it is demonstrated that non-axisymmetric instability modes prevail in a wide range of Q for conducting walls and axisymmetric oscillatory modes may, in fact, become more critical than both of the non-axisymmetric and axisymmetric stationary modes at higher values of the Hartmann number.

1. Introduction

The problem of the hydrodynamic stability of a viscous flow between two concentric rotating cylinders was first studied by Taylor (1923). He found experimentally that the flow becomes unstable when the speed of the inner cylinder exceeds some critical value. The instability produced a steady secondary motion in the form of cellular toroidal vortices, which we now call Taylor vortices, spaced regularly along the axis of the cylinder; his theoretical predictions were also in excellent agreement with his experiments. Other workers continued to investigate this important hydrodynamic stability phenomenon. In the early stages, Chandrasekhar (1954), DiPrima (1960) and Harris & Reid (1964) studied the linearized problem using different methods. In their theoretical analyses, the stability of the basic flow has been considered only with respect to axisymmetric disturbances. However, Nissan, Nardacci & Ho (1963) and Coles (1965) found from experiment that when the cylinders are counter-rotating, if the parameter μ which represents the angular velocities ratio of outer to inner cylinder is sufficiently negative, the critical instability mode for Couette flow may occur for non-

axisymmetric rather than axisymmetric disturbance. Krueger, Gross & DiPrima (1966) further considered the mathematical problem of the linear stability of Couette flow with respect to non-axisymmetric disturbances and made a complete investigation. Under small-gap approximation, they found that when $\mu \leqslant -0.78$ the critical Taylor number occurs for non-axisymmetric disturbances. Their theoretical predictions were also confirmed by the experimental work of Andereck, Lin & Swinney (1986).

A more complicated fundamental problem is the hydromagnetic stability of dissipative Couette flow, a viscous electrically conducting fluid moving between two concentric rotating cylinders in the presence of an applied axial magnetic field. This problem is also interesting because of its important applications for the gaseous core nuclear reactors and power-generating devices. The stability of this flow was first studied by Chandrasekhar (1953, 1961) under the assumptions of small-gap approximation and axisymmetric disturbance. Using variational and Galerkin expansion methods, he made a complete theoretical analysis and discussed the asymptotic behaviours of critical Taylor number and wavenumber when the Hartmann number Q approaches infinity. Kurzweg (1963) also considered this stability problem and found the relationships between the critical Taylor number, Hartmann number, and magnetic Prandtl number. However, his results are restricted to corotating cylinders and axisymmetric stationary mode. Roberts (1964) had derived the governing equations of non-axisymmetric disturbances for the finite-gap problem. Unfortunately, he only considered the case $\eta = 0.95$ (where η represents the ratio of the radius of inner cylinder to that of outer cylinder), $\mu = 0$, and non-conducting walls, in his paper. His analysis of non-axisymmetric disturbance was rather less complete. Chang & Sartory (1967) studied this problem with small-gap approximation, conducting cylinders and axisymmetric stationary and oscillatory modes. It was demonstrated by them that at sufficiently high magnetic field strength, axisymmetric oscillatory disturbances may become more critical than stationary disturbances. They also pointed out that it is still not known how the Hartmann number Q affects the stability behaviours of non-axisymmetric disturbances. Hassard, Chang & Ludford (1972) obtained an exact solution of this problem under several assumptions and restrictions. In addition, Donnelly & Ozima (1962) have performed experiments on hydromagnetic Couette flows of mercury between two long non-conducting cylinders for the case $\mu = 0$. Their results are in agreement with the theoretical predictions of Chandrasekhar (1961). Of particular interest are the experimental results of Donnelly & Caldwell (1964). By using stainless-steel cylinders, they found that a new instability may present which begins before the axisymmetric disturbance as the magnetic field is sufficiently large. The new instability is relatively weak compared to the other and they suggested that the mode of instability would be non-axisymmetric. A nonlinear stability analysis was given by Tabeling (1981) and Takhar, Ali & Soundalgekar (1989) further showed the amplitude of the radial velocity and the cell-pattern on graphs for axisymmetric disturbances and for both of the conducting and non-conducting walls with several different value of μ and Q.

In the present study, we consider the hydromagnetic stability of dissipative Couette flow within a small-gap coaxial cylinders. A complete linear stability analysis is implemented, in which three-dimensional disturbances of both stationary and oscillatory modes are considered. We first compare the numerical results with those of previous studies and discuss the instabilities at low and high Hartmann number separately. For low values of Q, it will be demonstrated that the onset mode will become the axisymmetric stationary mode when the Hartmann number Q exceeds some critical value which depends on the boundary conditions even though the value

of μ is sufficiently negative. The transition of the onset of instability from the non-axisymmetric mode ($m = 4$, where m represents the azimuthal wavenumber) to the axisymmetric stationary mode ($m = 0$) for $\mu = -1$ will also be shown in detail, and a systematic study which covers $-1.25 \leqslant \mu < 1$ is carried out. For high values of Q, we first show the region prevailed by non-axisymmetric instability modes in the plane (μ, Q) which covers $-1 \leqslant \mu < 1$ and $0 \leqslant Q \leqslant 10000$ for the case of conducting walls. Then results for three typical cases are reported. These belong to flow between (i) a rotating inner wall with a stationary outer wall, (ii) counter-rotating walls, and (iii) corotating walls. Note that if there is no magnetic field applied, this problem reduces to the general Couette flow and has been solved by Krueger *et al.* (1966). It has been mentioned that they found that when $\mu \leqslant -0.78$, the onset mode is non-axisymmetric. However, for hydromagnetic dissipative Couette flow, how the magnetic field affects the stability behaviours of non-axisymmetric disturbances is what we want to investigate. From a purely mathematical point of view such an investigation is also necessary to complete the analysis of the stability of this problem. The onset of non-axisymmetric instability may lead to a spiral structure or a 'ribbon' which means the flow is azimuthally periodic and the full pattern rotates solidly with an angular velocity (see Chossat & Iooss 1994). In the present paper as well as the results of Krueger *et al.* (1966), the onset of non-axisymmetric instability mode indicates that the instability leads to a weak spiral vortex motion as observed by Coles (1965, p. 399) in circular Couette flow.

2. Problem formulation and method of solution

Let r, θ and z denote the usual cylindrical polar coordinates, and let u_r, u_θ, and u_z and H_r, H_θ, and H_z denote the components of velocity and of the magnetic field intensity, respectively. We consider two infinitely long concentric circular cylinders with the z-axis as their common axis and let the radii and angular velocities of the inner and outer cylinders be R_1, R_2 and Ω_1, Ω_2, respectively. The equations of motion for a viscous, electrically conducting incompressible fluid in the presence of a uniform magnetic field in the axial direction admit a steady solution,

$$\left.\begin{aligned} u_r = u_z = 0, \quad u_\theta = V(r) = Ar + B/r, \\ H_r = H_\theta = 0, \quad H_z = H = \text{constant}, \end{aligned}\right\} \tag{1}$$

where

$$A = \frac{\mu - \eta^2}{1-\eta^2}\Omega_1, \quad B = \frac{R_1^2(1-\mu)}{1-\eta^2}\Omega_1. \tag{2}$$

To study the stability of this flow we superimpose a general disturbance on the basic solution, substitute it in the governing equations and neglect quadratic terms in the usual way. Since the coefficients in the resultant disturbance equations depend only on r, it is possible to look for solutions of the form

$$u_\theta = V(r) + v(r)\exp[st + \mathrm{i}(m\theta + \lambda z)], \tag{3}$$

where $v(r)$ is the azimuthal component of the small disturbance velocity, and with similar expressions for the other components of velocity, the pressure, and the components of magnetic field intensity. It is assumed that λ be real and m be an integer. Without loss of generality, we can take m to be zero or a positive integer. The parameter s will be complex in general. In the present analysis we will be concerned

with the small-gap case in which the gap $d = R_2 - R_1$ is small compared to R_1 so that terms $O(d/R_1)$ can be neglected. The derivation of the small-gap equations is essentially the same as for the classical hydromagnetic dissipative Couette flow (see Chandrasekhar 1961) except that now we must also consider terms involving differentiation with respect to the circumferential coordinate θ. The proper scaling for θ has been discussed by Krueger *et al.* (1966) and need not be repeated here.

We now introduce the dimensionless variables

$$\left.\begin{aligned} r = R_1 + xd, \quad \delta = \frac{d}{R_1}, \quad a = \lambda d, \quad \sigma = \frac{sd^2}{\nu}, \\ k = \left(-\frac{\Omega_1}{4A}\right)^{1/2} m, \quad T = -\frac{4A\Omega_1 d^4}{\nu^2}, \quad Q = \frac{\mu_0 H^2 d^2}{4\pi\rho\nu\epsilon}, \end{aligned}\right\} \tag{4}$$

where ν, μ_0, and ϵ represent kinematic viscosity, magnetic permeability and electric resistivity, respectively. Since the small-gap approximation yields $A = -\Omega_1(1-\mu)/2\delta$ plus terms $O(1)$, we have asymptotically

$$k \sim [\delta/2(1-\mu)]^{1/2} m, \quad T \sim 2(1-\mu)(\Omega_1 R_1 d/\nu)^2 \delta, \tag{5}$$

which account for the scaling of the azimuthal wavenumber and the Taylor number, respectively. Under terrestrial conditions, we let the ratio ν/ϵ be small (see also Chandrasekhar 1961). After combining the governing equations of perturbations, we obtain the following eighth-order system of ordinary differential equations:

$$[\mathrm{L}(\mathrm{D}^2 - a^2) + Qa^2]\, u = -a^2 T\Omega(x)(\mathrm{D}^2 - a^2)\,\psi, \tag{6}$$

$$[\mathrm{L}(\mathrm{D}^2 - a^2) + Qa^2]\,\psi = u, \tag{7}$$

where

$$\mathrm{D} = \mathrm{d}/\mathrm{d}x, \quad \mathrm{L} = \mathrm{D}^2 - a^2 - \sigma - \mathrm{i}kT^{1/2}\Omega(x), \quad \Omega(x) = 1 - (1-\mu)x, \tag{8}$$

and ψ represent the azimuthal component of the small disturbance magnetic field. The appropriate boundary conditions at $x = 0$ and $x = 1$ for non-conducting walls are

$$u = \mathrm{D}u = \psi = (\mathrm{D}^2 - a^2)\,\psi = 0, \tag{9}$$

and for conducting walls are

$$u = \mathrm{D}u = \mathrm{D}\psi = (\mathrm{D}^2 - a^2)\,\psi = 0. \tag{10}$$

A detailed discussion and derivation for equations (9) and (10) could be found in Chandrasekhar (1961). The homogeneous set of equations (6) and (7) with the boundary conditions (9) or (10) determine an eigenvalue problem of the form

$$F(\mu, Q, k, a, \sigma, T) = 0. \tag{11}$$

The marginal state is characterized by the real part of σ, σ_r, equal to zero. For given values of μ and Q, which determine the basic state velocity and magnetic field strength, we seek the minimum real positive T over real $k \geqslant 0$, for which there is a solution for (11) with $\sigma_r = 0$. The value of T sought is the critical Taylor number T_c for assigned values of μ and Q. The values of a and k corresponding to T_c determine the form of the critical disturbance. Note that it has physical meaning only for values of k corresponding to integer values of the azimuthal wavenumber m, and under the small-gap approximation we choose $\delta = 0.05$ for the present study. Moreover, the imaginary part of σ, namely σ_i, corresponding to T_c determines the frequency of the oscillation.

	Non-conduction walls			
	a_c		T_c	
Q	(A)	(B)	(A)	(B)
0	4.00	4.0	18662	18700
10	3.98	4.0	23052	23100
100	3.39	3.40	71497	71620
1000	0.99	0.96	714388	714300
10000	0.31	0.29	7245596	7248000
	Conduction walls			
	a_c		T_c	
Q	(A)	(B)	(A)	(B)
0	4.00	4.0	18662	18700
10	4.17	3.9	24391	24570
30	4.36	4.3	36845	36930
100	4.70	4.7	91851	92000
1000	4.93	4.9	1803197	1795000

TABLE 1. Comparison between the results of present study (A) and those of Chandrasekhar (B) (1961) for axisymmetric stationary mode $m = 0$ and $\mu = -1$.

For a fixed z, the wave will propagate in the direction of the basic flow with an angular velocity given by $c = -s_i/m\Omega_1 = -\sigma_i/kT^{1/2}$. Then we solve the two-point eigenvalue problem defined by (6)–(10) by a shooting technique together with a unit-disturbance method. Indeed, there are many analytical methods which can be used in the stability analysis for non-axisymmetric disturbances, for example, the work done by Weinstein (1977*a*, *b*) for wavy vortices in the flow between two long eccentric rotating cylinders. The method in the present study has also been widely used by several workers for similar hydrodynamic stability problems (see DiPrima 1955; Harris & Reid 1964; Sparrow, Munro & Jonsson 1964; Krueger, Gross & DiPrima 1966; Chen & Chang 1992). For details, the reader is referred to Krueger *et al.* (1966). In order to obtain a faster convergence of the iteration, we use a modified algorithm developed by Chen & Chang (1992) for this eigenvalue problem.

3. Results and discussion

3.1. *Verification of computer code*

Chandrasekhar (1961) studied the instability of hydromagnetic dissipative Couette flow with respect to axisymmetric disturbances, which is a special case of the present study with $m = 0$. So we conduct calculations for $m = 0$ and check the results in terms of T_c and a_c for both non-conducting and conducting walls with the corresponding data obtained by Chandrasekhar (table 1). The comparison is in good agreement. Another check is made by considering the instability of Taylor flow against non-axisymmetric disturbance as carried out by Krueger *et al.* (1966). By assuming $Q = 0$, we obtain the critical values T_c, a_c and σ_i for various m, which are also in excellent agreement with those of Krueger *et al.* (see table 2 and figure 3*a*).

Q	m	a_c	T_c	$-\sigma_i$	c
0	0	4.00	18662	0	0
	1	3.94	18472	6.3281	0.4164
	2	3.80	17965	12.125	0.4046
	3	3.68	17400	16.984	0.3838
	4	3.65	17126	21.257	0.3632
	5	3.69	17343	25.483	0.3460
	6	3.79	18169	30.536	0.3377
20	0	3.94	27666	0	0
	1	3.89	27542	7.7599	0.4181
	2	3.76	27202	15.112	0.4098
	3	3.61	26827	21.733	0.3956
	4	3.57	26843	27.860	0.3802
	5	3.65	27620	34.096	0.3670
	6	3.81	29392	41.676	0.3624
45	0	3.80	40128	0	0
	1	3.76	40110	9.4226	0.4208
	2	3.65	40063	18.611	0.4158
	3	3.51	40130	27.369	0.4073
	4	3.49	40784	35.551	0.3936
	5	3.63	42586	44.812	0.3885
	6	3.86	45819	55.711	0.3879
50	0	3.77	42770	0	0
	1	3.73	42776	9.7536	0.4218
	2	3.62	42797	19.296	0.4171
	3	3.49	42971	28.319	0.4072
	4	3.47	43787	37.121	0.3966
	5	3.62	45827	46.951	0.3923
	6	3.88	49373	58.516	0.3925

TABLE 2. The critical value of T_c and the corresponding values of a_c, σ_i, and c for assigned values of Q and m for $\mu = -1$ at low Hartmann number (non-conduction walls).

3.2. *Stability characteristics at low Hartmann number*

We first study the transition of the onset of instability for $\mu = -1$ and then discuss the general stability characteristics at low values of Q. For $Q = 0$ and $\mu = -1$, the onset mode is non-axisymmetric with azimuthal wavenumber $m = 4$ disregarding whether the boundary conditions are conducting or non-conducting walls. It is the purpose of present study to investigate what will happen to the onset of instability as the magnetic field strength increases in the axial direction. Calculations have been performed for $0 \leqslant Q \leqslant 100$ and the resolution of ΔQ is up to 1. In table 2 the critical values of T_c and a_c, as well as the corresponding values of the dimensionless frequency σ_i, and the dimensionless angular wave velocity c are tabulated for $Q = 0$, 20, 45, and 50 and a suitable range of assigned value of m for non-conducting walls and $\mu = -1$. In table 3 the same critical values are also tabulated for $Q = 10$, 20, 26, and 30 for conducting walls. From these tables, we observe that the critical Taylor number T_c increases with the strength of the magnetic field. This indicates that the presence of a magnetic field for a viscous, conducting fluid is a stabilizing effect. And for the same Q, the T_c for conducting walls is always higher than non-conducting walls which means the flow remains more stable between conducting walls. In particular, we find that the critical disturbance is no longer the non-axisymmetric mode with $m = 4$ when the parameter Q increases and the transition of the onset mode occurs with decreasing azimuthal wavenumber m simultaneously. Then the non-axisymmetric travelling waves

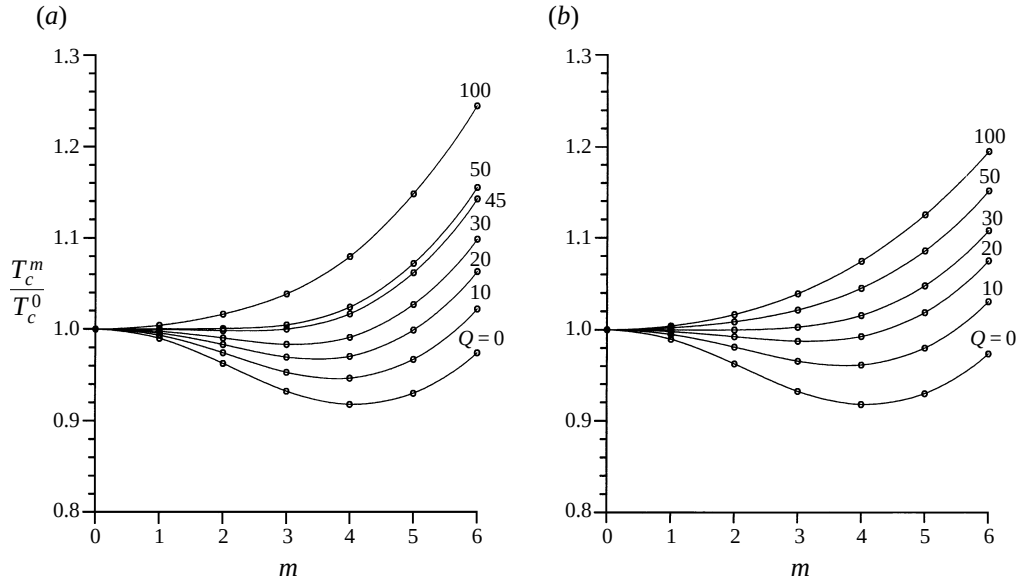

FIGURE 1. The variation of T_c^m/T_c^0 for assigned values of Q and $\mu = -1$ (*a*) non-conducting walls, (*b*) conducting walls.

Q	m	a_c	T_c	$-\sigma_i$	c
10	0	4.17	24391	0	0
	1	4.13	24269	7.1585	0.4109
	2	4.02	23935	13.960	0.4035
	3	3.90	23555	20.113	0.3906
	4	3.85	23441	25.568	0.3734
	5	3.88	23898	31.062	0.3593
	6	3.98	25138	37.562	0.3532
20	0	4.28	30439	0	0
	1	4.25	30378	7.9614	0.4085
	2	4.17	30218	15.667	0.4031
	3	4.07	30069	22.855	0.3929
	4	4.02	30214	29.647	0.3814
	5	4.05	30997	36.482	0.3706
	6	4.16	32717	44.523	0.3669
26	0	4.33	34243	0	0
	1	4.30	34218	8.4391	0.4079
	2	4.24	34157	16.663	0.4032
	3	4.16	34163	24.544	0.3959
	4	4.11	34491	32.147	0.3870
	5	4.14	35501	39.861	0.3784
	6	4.25	37524	48.367	0.3722
30	0	4.36	36853	0	0
	1	4.34	36850	8.7556	0.4079
	2	4.28	36856	17.321	0.4034
	3	4.21	36967	25.596	0.3969
	4	4.17	37425	33.641	0.3888
	5	4.20	38596	41.848	0.3811
	6	4.31	40835	51.468	0.3796

TABLE 3. The critical value of T_c and the corresponding values of a_c, σ_i, and c for assigned values of Q and m for $\mu = -1$ at low Hartmann number (conduction walls).

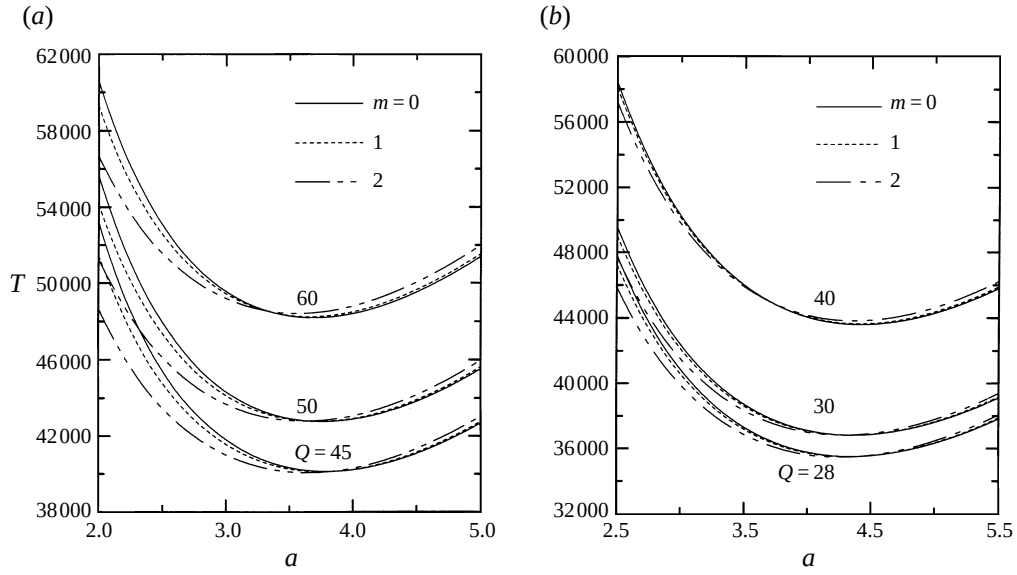

FIGURE 2. Neutral curves of different modes for $\mu = -1$ and various Q (*a*) non-conducting walls, (*b*) conducting walls.

will disappear when the value of Q exceeds some critical value and the critical disturbance becomes the axisymmetric stationary mode. This critical value is 49 for non-conducting walls and 31 for conducting walls.

In our calculations corresponding to the ranges $0 \leqslant Q < 20$, $20 \leqslant Q < 42$, $42 \leqslant Q < 49$, $49 \leqslant Q$, the critical Taylor number is determined by disturbances with $m = 4$, 3, 2, and 0, respectively, for non-conducting walls. Similarly, for conducting walls, as Q is in the ranges $0 \leqslant Q < 15$, $15 \leqslant Q < 26$, $26 \leqslant Q < 30$, $Q = 30$, $30 < Q$, the T_c is determined by disturbances with $m = 4$, 3, 2, 1 and 0, respectively. To interpret the results in as simple a manner as possible, we denote the appropriate Taylor number by T_c^m. In figure 1 (*a*), the values of T_c^m/T_c^0 for different values of m are given for several values of Q. Note that for non-conducting walls, $Q = 0$, 10, 20, 30, and 45, the critical value of T corresponds to a non-axisymmetric disturbance with 4, 4, 3, 3, and 2 waves in the azimuthal direction, respectively. When Q exceeds 49, the critical value of T then corresponds to an axisymmetric disturbance with $m = 0$. The similar transition process is shown in figure 1 (*b*) for conducting walls. For $Q = 0$, 10, 20, and 30, the critical disturbances are non-axisymmetric with $m = 4$, 4, 3, and 1, respectively. The stability of this flow is dominated by axisymmetric disturbance again when Q is greater than 30.

Now we pay attention to the transition of the critical wavenumber a_c in the axial direction as Q increases. For non-conducting walls, $Q = 0$, 10, 20, 30, 45, and 50, the corresponding values of a_c are 3.65, 3.61, 3.61, 3.58, 3.65, and 3.77, respectively. This indicates the critical axial wavelength $2\pi d/a_c$ for which non-axisymmetric disturbances occur will be slightly increased and then slightly decreased. When Q exceeds 49, a_c will decrease gradually as found by Chandrasekhar (1961). In the other case, for conducting walls, we can easily observe from table 3 that a_c is generally a monotone increasing function of Q. We also find that the wavenumber of the onset mode is not always shortest in the axial direction among different m-modes. In the cases for which non-axisymmetric disturbances dominate the instability of this flow, the critical axial wavelength will be slightly greater than the value predicted for an axisymmetric disturbance at that value of Q.

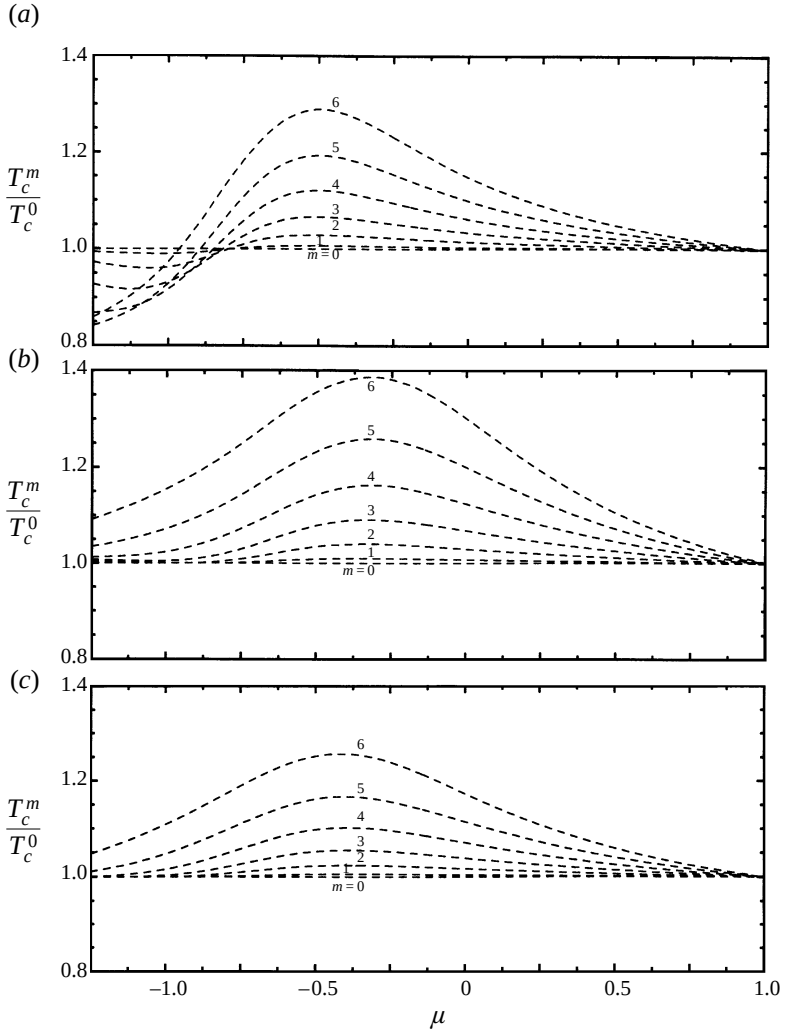

FIGURE 3. The variation of T_c^m/T_c^0 with μ for assigned values of m (*a*) $Q = 0$, (*b*) $Q = 50$ (non-conducting walls), (*c*) $Q = 30$ (conducting walls).

Some further discussion must be made for Q near the critical value. The neutral curves in the (T, a)-plane of modes $m = 0$, 1 and 2 for various Q are shown in figure 2(*a*) for non-conducting walls and 2(*b*) for conducting walls. We observe that the three modes become critical simultaneously when Q approaches the critical value. This explains why there is no occurrence of the $m = 1$ mode as Q nears 50 for non-conducting walls and the $m = 1$ mode may exist only at $Q = 30$ for conducting walls. The possibility of three-mode interaction may play an important role in the nonlinear regime. It is probable that with slightly increasing T above T_c, several equilibrium states are attained. To resolve such problems it is necessary to consider the nonlinear equations. We also note that it corresponds to a finite jump of a_c when the onset mode is changing.

To study the general stability characteristics of hydromagnetic dissipative Couette flow, we consider $-1.25 \leqslant \mu < 1$ since μ is the main parameter determining the basic flow. In figure 3(*a*), the variation of T_c^m/T_c^0 with μ for assigned values of m and $Q = 0$

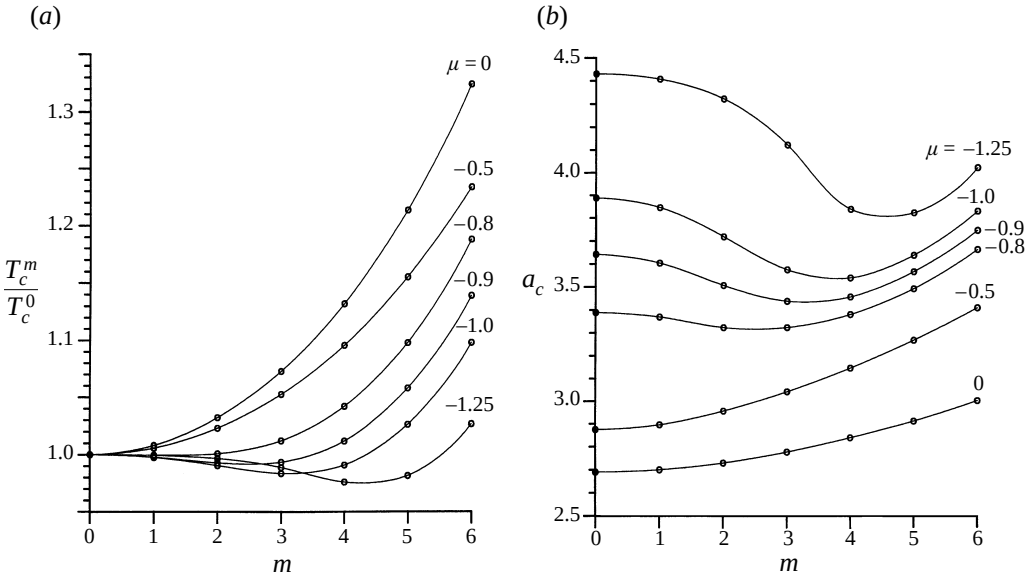

FIGURE 4. (*a*) The variation of T_c^m/T_c^0 with m for assigned values of μ and $Q = 30$ for non-conducting walls. (*b*) The variation of a_c with m for assigned values of μ and $Q = 30$ for non-conducting walls.

is shown. This figure is the same as that obtained by Krueger *et al.* (1966) for the Taylor problem. We reproduce it in order to compare with figure 3(*b*) for non-conducting walls with $Q = 50$ and figure 3(*c*) for conducting walls with $Q = 30$. For a given value of μ, the critical Taylor number is given by the lowest point on the set of curves. We first examine figure 3(*a*), it is found that there is a critical value of μ, approximately -0.78, above which the critical disturbance is axisymmetric and below which it is non-axisymmetric. We denote this critical value of μ as μ_c. Further, the instability mode is non-axisymmetric with $m = 1$ at $\mu = -0.78$ and changes into other modes with higher m as μ decreases. We now examine figures 3(*b*) and 3(*c*). They both reveal that, for fixed μ, the critical disturbance becomes the axisymmetric stationary mode when Q is greater than some value even though the value of μ is sufficiently negative. We call this the critical value of Q and denote it by Q_c. The critical Hartmann numbers for non-conducting walls are 42, 49, 52, and 42 and for conducting walls are 30, 31, 29, and 18, for $\mu = -1.25$, -1, -0.9, and -0.8, respectively. In other words, the domain of Q in which non-axisymmetric modes prevail is limited and the instability of this flow will be dominated by axisymmetric disturbance if the magnetic field is sufficiently strong. However, for the case of conducting walls, it was demonstrated by Chang & Sartory (1967) that at sufficiently high Hartmann number, axisymmetric oscillatory disturbances may become more critical and an abrupt change of the wavenumber a_c may occur. So it is necessary to study further whether non-axisymmetric disturbances may be more critical or not at high Hartmann number. This point will be discussed in detail later. The critical values of Q for several assigned values of μ, where $\mu < -0.78$ which we have given, also indicate that the critical value of μ depends on Q. Both of the critical values Q and μ, Q_c and μ_c, are functions of each other, i.e. $Q_c = Q_c(\mu)$ and $\mu_c = \mu_c(Q)$. For non-conducting walls, the critical value μ_c is still about -0.78 as $Q < 40$. For example, figure 4(*a*) illustrates the values of T_c^m/T_c^0 for different values of m and several values of μ as $Q = 30$. We observe that for $\mu = -1.25$, -1.0, -0.9, and -0.8, the critical value of T corresponds to a non-axisymmetric disturbance with 4, 3,

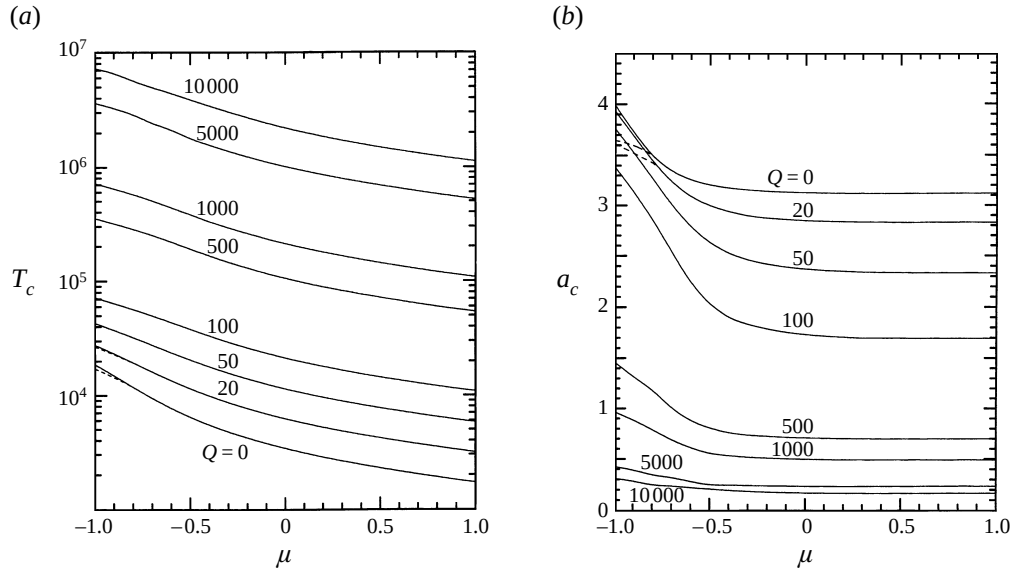

FIGURE 5. (*a*) The variation of T_c with μ for assigned values of Q (non-conducting walls); ——, axisymmetric stationary mode; – – –, non-axisymmetric mode. (*b*) The variation of a_c with μ for assigned vaues of Q (non-conducting walls); ——, axisymmetric stationary mode; – – –, non-axisymmetric mode.

2, and 1 waves travelling in the azimuthal direction, respectively. The corresponding critical values of a, a_c for different values of m and assigned values of μ are shown in figure 4(*b*). We find in the cases for which the onset mode is non-axisymmetric, the corresponding critical value of a is less than that for an axisymmetric disturbance. When the Hartmann number Q is above 40, μ_c will decrease slightly near -0.9 and then disappear because the instability of this flow will be dominated by the axisymmetric stationary mode, as we have shown. Note that the variation of T_c between the modes $m = 0$, 1, and 2, as $\mu = -0.9$ and Q is in the neighbourhood of 50, is still very small. For conducting walls, μ_c will decrease gradually near -0.9 with increasing Q and then disappear when Q is approximately greater than 30, which is similar to the results for non-conducting walls.

The variation of T_c and a_c versus varying μ for several assigned values of Q are given in figure 5 for non-conducting walls and in figure 6 for conducting walls, respectively. We first pay attention to the cases of low Hartmann number, and those of high Hartmann number will be discussed in §3.3. As shown in figures 5(*a*) and 6(*a*), T_c is generally a monotonic increasing function of Q for all the μ considered. This means that the applied magnetic field always has a stabilizing effect on this flow. The critical Taylor number for the non-axisymmetric disturbance is lower than that for the axisymmetric disturbance initially as $Q = 0$ and $\mu < -0.78$, and then T_c for axisymmetric stationary mode becomes lower than that for non-axisymmetric mode when Q is large enough for all the range of μ considered. We also find that T_c of the conducting case is higher than that of the non-conducting case for the same Q and μ which indicates the effect of Q is stronger in the conducting walls. Note that when Q approaches the critical value $Q_c(\mu)$ and μ is less than $\mu_c(0)$, the differences of T_c for axisymmetric and non-axisymmetric disturbances become smaller gradually. For instance, for the case of $\mu = -1$, $Q = 20$ and conducting walls, the critical value of the Taylor number occurs for $m = 3$ and $T_c^3 = 30069$. At the same time, T_c for $m = 0$ is

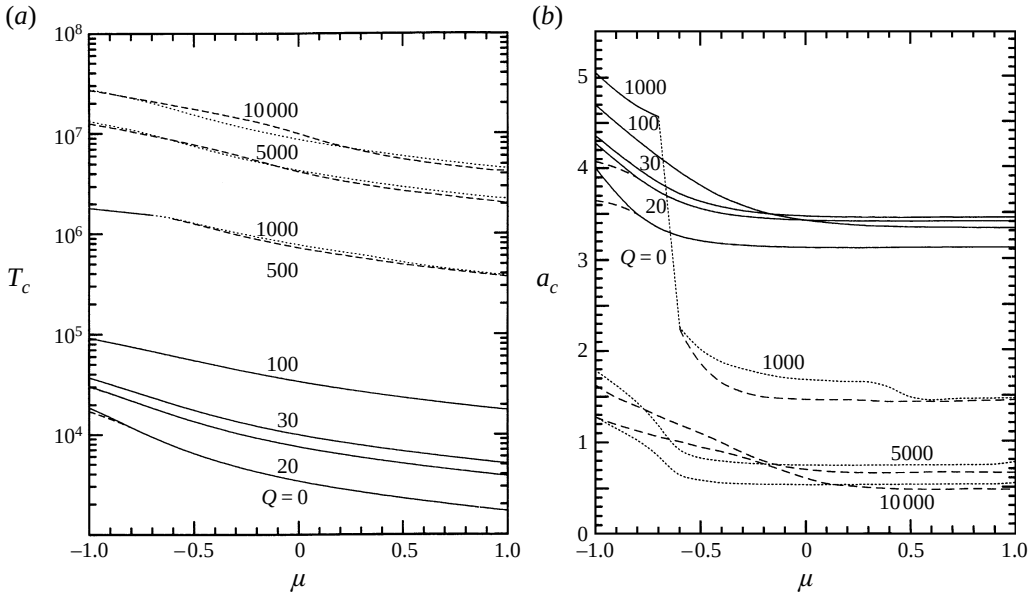

FIGURE 6. (*a*) The variation of T_c with μ for assigned values of Q (conducting walls); ——, axisymmetric stationary mode; ---, axisymmetric oscillatory mode; –––, non-axisymmetric mode. (*b*) The variation of a_c with μ for assigned values of Q (conducting walls); ——, axisymmetric stationary mode; ---, axisymmetric oscillatory mode; –––, non-axisymmetric mode.

$T_c^0 = 30439$. For $\delta = 0.05$, the critical value of the Reynolds number $R = R_1 \Omega_1 d/\nu$ could be obtained by equation (5) and we have $(R_c^0 - R_c^3)/R_c^0 \sim 0.0061$, which indicates that the difference in the critical speed of the inner cylinder is a small percentage change. For $\mu = -0.9$ and $\mu = -0.8$, the changes are even smaller. Such small differences are probably within the limits of experimental errors. Thus, it may be that the onset of instability could not be detected by critical speed measurements alone. It also would be necessary to carry out more detailed experimental work concerning the critical state and the subsequent growth of the disturbance for the cases where μ is less than $\mu_c(0)$.

Figure 5(*b*) illustrates that a_c decreases monotonically with Q for non-conducting walls and all the μ considered. In other words, elongated Taylor cells will be observed for large Q. On the other hand, figure 6(*b*) illustrates that, at first, a_c increases monotonically with Q for conducting walls, and Taylor cells have a shorter wavelength in the axial direction for large Q. We should bear in mind that the range of Q which we consider here is not wide. The relationships between a_c and Q are more complex at high values of the Hartmann number for the case of conducting walls. We also note that when μ is less than the critical value, a_c for the non-axisymmetric mode is always less than the value predicted for the axisymmetric stationary mode.

3.3. *Stability characteristics at high Hartmann number*

To study the stability characteristics of this flow at high values of Q, we consider wide ranges of μ and Q which are the two major parameters determining the basic state. Calculations have been performed for $-1 \leqslant \mu < 1$ and $100 \leqslant Q \leqslant 10000$. The resolutions of both $\Delta\mu$ and ΔQ are up to 0.1 and 10, respectively. Results for several typical cases with assigned values of μ are discussed in further detail. For the case of non-conducting walls, as we have shown previously, the non-axisymmetric instability

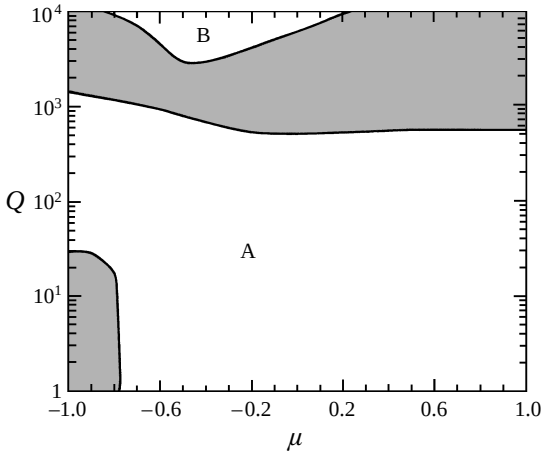

FIGURE 7. Areas of different critical disturbances prevail in the (μ, Q)-plane for conducting walls. The shaded area represents non-axisymmetric mode; section A is axisymmetric stationary mode and section B is axisymmetric oscillatory mode.

modes prevail only in a limited range of Q when μ is sufficiently negative. The critical disturbance is always the axisymmetric stationary mode even though the Hartmann number is very high. However, for the case of conducting walls, the results are quite different. In figure 7, the shaded area in the plane (μ, Q) represents where non-axisymmetric instability modes prevail and is bounded by sections A and B. It is found that the flow instability is dominated by non-axisymmetric disturbances in a wide range of Q for all the μ considered. The shaded area at the left-hand lower corner has been studied in the previous discussion. Section A represents the area where the critical disturbance is the axisymmetric stationary mode and the section B is the axisymmetric oscillatory mode. The lower boundary value of Q of the upper shaded area first decreases with μ, reaches a minimum near $\mu = 0$, then increases slightly and tends to be a constant as $\mu \geqslant 0.5$. On the other hand, the upper boundary value of Q also first decreases with μ, reaches a minimum near $\mu = -0.5$, then increases rapidly. This illustrates that the domain of Q, in which non-axisymmetric modes prevail, depends heavily on μ and has a minimum near $\mu = -0.5$, as shown.

For a given value of μ, typically as $\mu = 0$, a rotating inner wall with a stationary outer wall, the onset of instability is the axisymmetric stationary mode at low or moderate strength of axial magnetic field and becomes the non-axisymmetric mode when the value of Q is above the lower critical value 510. If Q increases further and is greater than the upper critical value 6080, the instabilities of this flow will be dominated by axisymmetric oscillatory modes. In order to illustrate the transition process of the onset of instability, it is necessary to investigate the nature of the neutral curves in the plane (T, a). Chang & Sartory (1967) have presented the results of the neutral curves of axisymmetric disturbances including stationary and oscillatory modes for conducting walls with selected typical cases. Here we further take the neutral curve of the most critical non-axisymmetric mode into consideration. In general, a neutral stability diagram is multiple valued at a given value of Q. For instance, at $Q = 510$, the two lowest branches of the neutral curves for axisymmetric stationary modes are shown by the circle–solid curves in figure 8(*a*). As $Q < 510$, it is found that the critical Taylor number T_c and wavenumber a_c are dertermined by the minimum of the lower branch of axisymmetric stationary mode. At $Q = 510$, both of the neutral curves for non-axisymmetric mode $m = 1$ and the lower branch for axisymmetric stationary mode

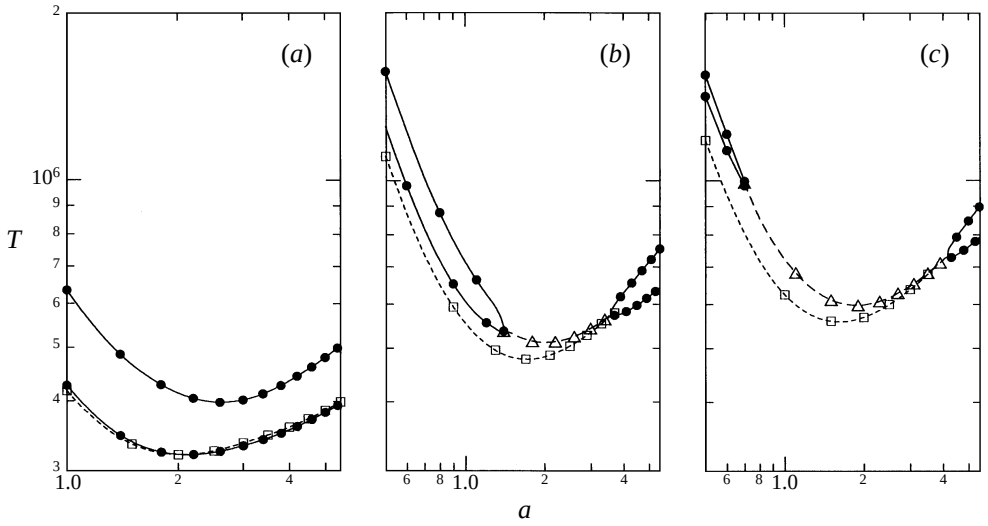

FIGURE 8. Neutral curves for conducting walls with $\mu = 0$ and various Q; —●—, axisymmetric stationary mode; —△—, axisymmetric oscillatory mode; —□—, non-axisymmetric mode $m = 1$; (*a*) $Q = 510$, (*b*) 700, (*c*) 800.

become critical simultaneously. When Q increases further, the two branches of the neutral curve for the axisymmetric stationary mode begin to converge and finally intersect and break into two separate loops with a gap between them. Simultaneously, axisymmetric oscillatory modes appear and lie between the two loops. Figure 8(*b*) illustrates such a result for $Q = 700$ and the axisymmetric oscillatory mode is shown by the triangle–dash curve. We observe that the left-hand loop for the axisymmetric stationary mode has a lower minimum than the right-hand loop and the minimum of the neutral curve for axisymmetric oscillatory modes is even lower than that of the left-hand loop, but now T_c is determined by the non-axisymmetric mode with $m = 1$. In our detailed calculations, we find that the minimum of the left-hand loop is almost equal to that of the axisymmetric oscillatory mode at $Q = 670$. Note that, at first, the left-hand loop is more critical than the right. Chang & Sartory (1967) found that the two loops begin to rise and recede to the left and to the right of the wavenumber a with increasing Q. The left-hand loop rises more rapidly than the right-hand loop and the minima of the two loops become equal at $Q = Q^* = 730$. As $Q > 730$, the right-hand loop will become more critical than the left-hand loop, as shown in figure 8(*c*) for $Q = 800$. The neutral curve of the axisymmetric oscillatory mode still lies between the two loops and extends with increasing Q, the corresponding minimum of T is apparently lower than that of the right-hand loop. However, we find the critical disturbance is also non-axisymmetric mode with $m = 1$.

The domain of Q in which the non-axisymmetric mode $m = 1$ prevails is approximately $510 \leqslant Q \leqslant 6080$, as mentioned. When Q is above 6080, the onset of instability will be the axisymmetric oscillatory mode. To interpret this result, we consider further the transition of the neutral curves for counter-rotating walls with $\mu = -0.5$, as shown in figure 9. Chang & Sartory (1967) have shown that the axisymmetric stationary curves for the lowest two branches again intersect as Q is increased, but the initial point of intersection occurs near wavenumber $a = 0$. Thus, the neutral curve of the axisymmetric stationary mode consists of a single loop at sufficiently large values of Q, as shown in figure 9(*a*). They also found that, when Q

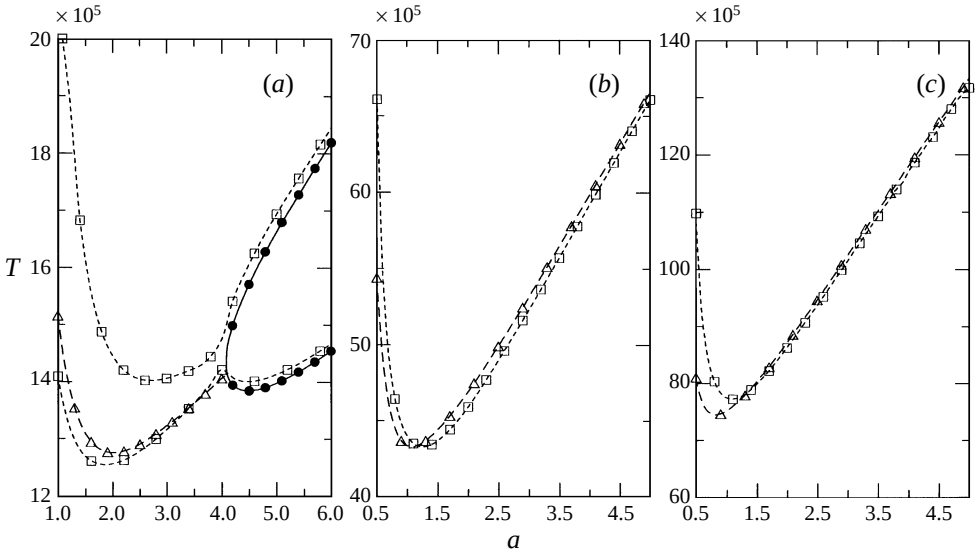

FIGURE 9. Neutral curves for conducting walls with $\mu = -0.5$ and various Q; —●—, axisymmetric stationary mode; —△—, axisymmetric oscillatory mode; —□—, non-axisymmetric mode $m = 1$; (*a*) $Q = 1000$, (*b*) 2990, (*c*) 5000.

is sufficiently large, there exist axisymmetric oscillatory disturbances which may become more critical than the stationary disturbances. As shown in figure 9(*a*) for $Q = 1000$, the axisymmetric oscillatory curve is more critical than the axisymmetric stationary loop, but now we find the critical disturbance should be the non-axisymmetric mode $m = 1$. Note that the two lowest branches of the neutral curves for $m = 1$ are shown and the lower branch has two local minima. The critical state is determined by the left-hand minimum. As Q is increased, the axisymmetric stationary loop and the right-hand local minimum of the lower branch for $m = 1$ rise and recede to the right-hand side quickly and the difference of T_c between the axisymmetric oscillatory mode and the non-axisymmetric mode $m = 1$ becomes smaller gradually. At $Q = 2900$, as shown in figure 9(*b*), both of the minima of axisymmetric oscillatory mode and non-axisymmetric mode $m = 1$ become approximately equal. As Q is greater than 2990, for example, at $Q = 5000$ is shown in figure 9(*c*), the critical disturbance becomes an axisymmetric oscillatory mode. The upper branch for $m = 1$ is omitted in figure 9(*b*, *c*) because this branch never becomes critical.

Figure 10 illustrates the transition of the neutral curves for the case $\mu = -1$. In figure 10(*a*), the neutral curves of axisymmetric stationary and oscillatory modes are the same as those given by Chang & Sartory (1967). We find that T_c is still determined by the loop for the axisymmetric stationary mode at $Q = 1000$. We also note that the minimum of the lower branch for the non-axisymmetric mode $m = 1$ is slightly higher than that of the loop for the axisymmetric stationary mode. When Q increases further, the lower branch for $m = 1$ gradually appears to have two local minima. As a result, at $Q = 1430$, the left-hand minimum with lower critical axial wavenumber for $m = 1$ is almost equal to that of the loop for the axisymmetric stationary mode, as shown in figure 10(*b*). The right-hand minimum of the lower branch for $m = 1$ never becomes critical and rises and recedes to the right-hand side rapidly, as does the loop for the axisymmetric stationary mode with increasing Q. As $Q > 1430$, for example, at $Q = 3000$, the onset of instability is determined by the non-axisymmetric mode with

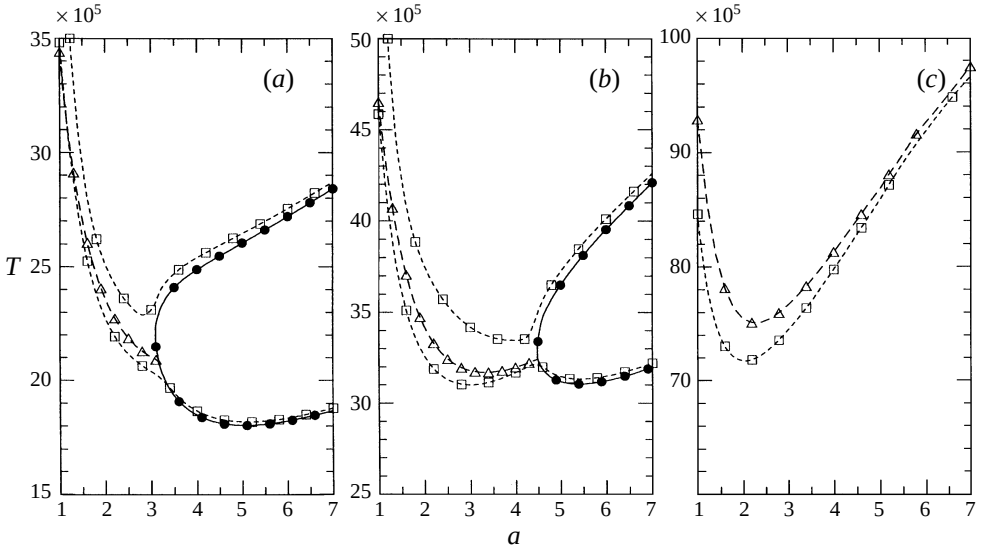

FIGURE 10. Neutral curves for conducting walls with $\mu = -1$ and various Q; —●—, axisymmetric stationary mode; —△—, axisymmetric oscillatory mode; —□—, non-axisymmetric mode $m = 1$; (*a*) $Q = 1000$, (*b*) 1430, (*c*) $Q = 3000$.

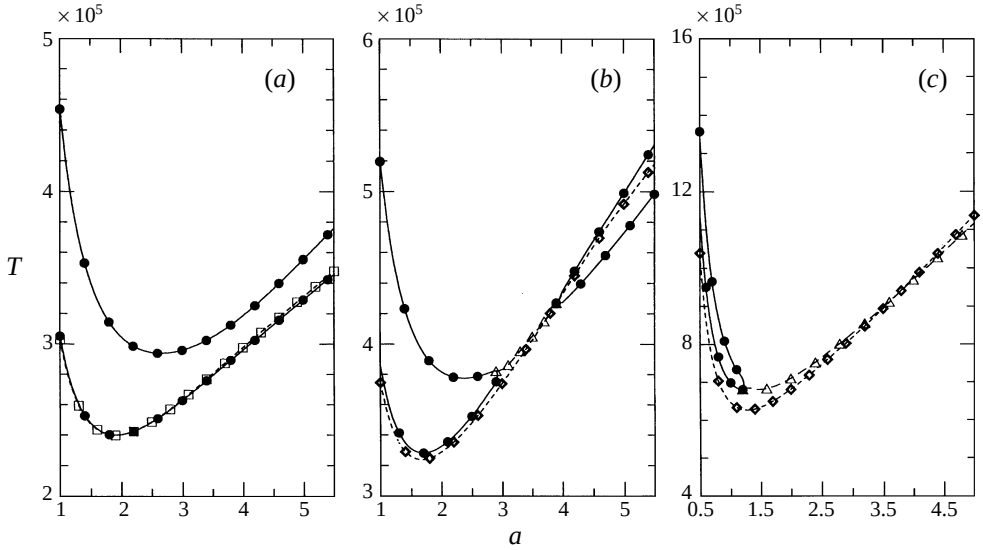

FIGURE 11. Neutral curves for conducting walls with $\mu = 0.5$ and various Q; —●—, axisymmetric stationary mode; —△—, axisymmetric oscillatory mode; —□—, non-axisymmetric mode $m = 1$; —◇—, non-axisymmetric mode $m = 2$; (*a*) $Q = 550$, (*b*) 700, (*c*) 1250.

$m = 1$. It is also found that at $Q = 1520$ both of the axisymmetric oscillatory and stationary modes become critical simultaneously and the oscillatory mode will be more critical than the stationary mode as $Q > 1520$. We could predict that the critical disturbance will finally become the axisymmetric oscillatory mode when Q is sufficiently large from the tendency of the upper boundary of the shaded area with decreasing μ, as shown previously in figure 7.

For the case of corotating conducting walls, the neutral curves of various Q are shown in figure 11 for $\mu = 0.5$. Chang & Sartory (1967) have discussed the neutral

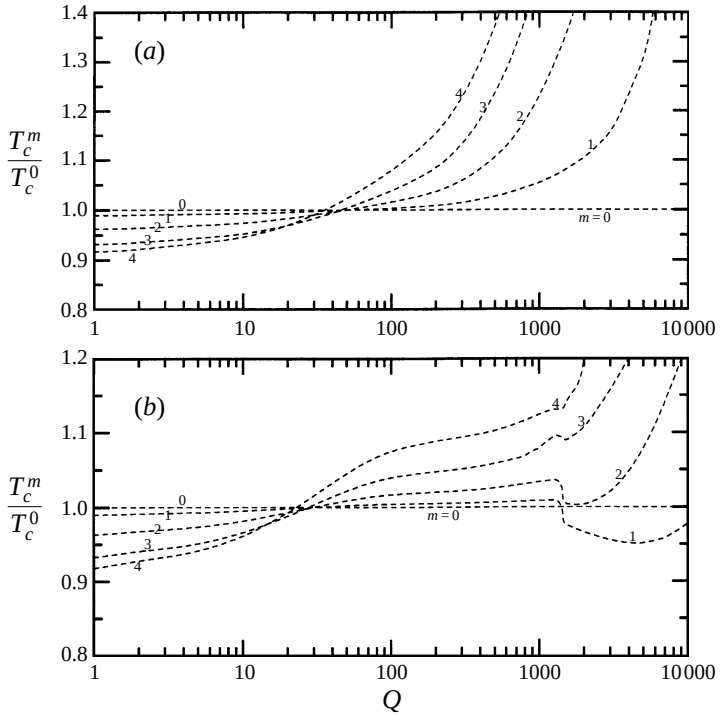

FIGURE 12. The variation of T_c^m/T_c^0 with Q for assigned values of m as $\mu = -1$ (*a*) non-conducting walls, (*b*) conducting walls.

curves for axisymmetric stationary modes and omitted the results for axisymmetric oscillatory modes, although they also found axisymmetric oscillatory modes occur for this case. As $Q < 550$, T_c is determined by the lowest branch of axisymmetric stationary modes. At $Q = 550$, the two lowest branches for axisymmetric stationary modes are shown in figure 11(*a*) and the minima for axisymmetric stationary mode and non-axisymmetric mode $m = 1$ become almost equal which is similar to the case $\mu = 0$ at $Q = 510$. As Q is increased, the intersection of the two branches for axisymmetric stationary modes occurs to the right of the minimum, and axisymmetric oscillatory modes appear and lie between the two loops as shown in figure 11(*b*). However, T_c is now determined by the non-axisymmetric mode with $m = 2$. When Q increases further, the two loops also begin to rise and recede to the left and right of *a* but now the right-hand loop rises more rapidly than the left. At $Q = 1250$, as shown in figure 11(*c*), we again observe that both the axisymmetric oscillatory and stationary modes become critical simultaneously, but T_c is still determined by the mode $m = 2$. Note that at first the range of Q in which the non-axisymmetric mode $m = 1$ prevails is narrow between $550 \leqslant Q \leqslant 600$, and the mode $m = 2$ prevails in $610 \leqslant Q \leqslant 2060$. As $Q > 2060$, the mode $m = 1$ becomes the onset mode again.

To demonstrate the transition of the critical disturbance more clearly, it is necessary to clarify how the magnetic field affects the stability behaviours of non-axisymmetric disturbances. Figure 12 illustrates the variation of T_c^m/T_c^0 with Q for several assigned values of m and $\mu = -1$. The most critical disturbance is the same determined by the lowest point on the set of curves for a given value of Q. Thus, for non-conducting walls as shown in figure 12(*a*), we find the onset of instability is the non-axisymmetric mode in the range $0 \leqslant Q < 50$ and the azimuthal wavenumber m gradually decreases with

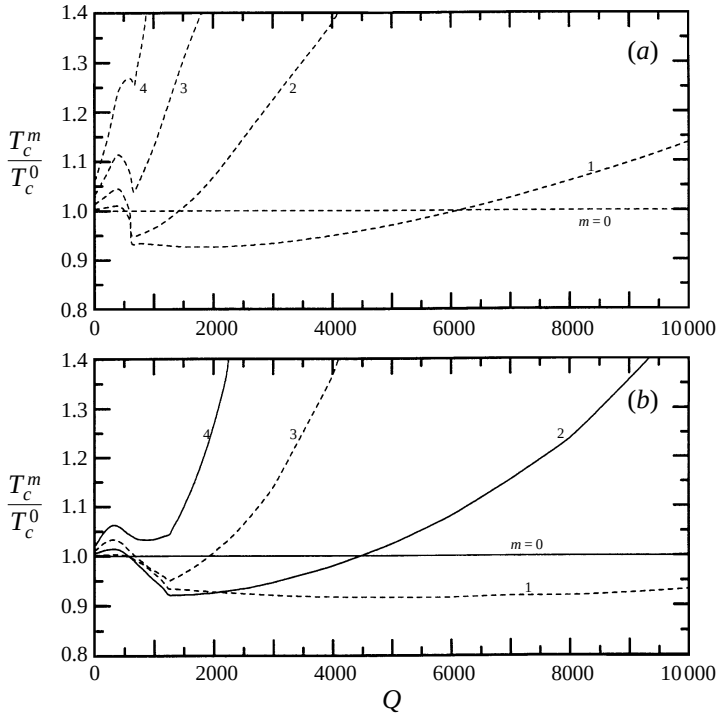

FIGURE 13. The variation of T_c^m/T_c^0 with Q for conducting walls with assigned values of m; (a) $\mu = 0$, (b) $\mu = 0.5$.

increasing Q, as we have discussed in detail for low Hartmann number. Moreover, it is apparent that the flow instability is always dominated by the axisymmetric stationary mode when Q is greater than 50. In comparison with non-conducting walls, figure 12(b) demonstrates the results for conducting walls. It is found that the stability behaviour of non-axisymmetric modes is similar to that of non-conducting walls at low Hartmann number, but quite different at high values of Q. As $Q > 30$, the ratios of T_c^m/T_c^0 for non-axisymmetric modes increase at first, experience a decreasing in a narrow range of Q which is due to the shift of the minimum of the neutral curve from the right-hand side to the left, for instance, as shown in figure 10(b). Then each curve shows a discontinuity in slope near $Q = 1520$ since the critical axisymmetric disturbance switches from stationary to oscillatory mode. In particular, we note that the critical disturbance becomes the non-axisymmetric mode with $m = 1$ again as $Q > 1430$ and the ratio for $m = 1$ gradually decreases with Q, reaches a minimum, then increases eventually for higher Q, so we could also predict that the onset of instability should be the axisymmetric oscillatory mode when Q is sufficiently large.

The variation of T_c^m/T_c^0 with Q for conducting walls are also presented in figure 13 for $\mu = 0$ and 0.5, respectively. We will not give the results for non-conducting walls at $\mu = 0$ and 0.5 because the critical disturbances are always axisymmetric stationary modes in these cases. As shown in figure 13(a), all the ratios for $m = 1$–4 initially increase with Q, then decrease, and each curve has a discontinuity in slope near $Q = 670$ which is also due to the switch from axisymmetric stationary to oscillatory mode. It is easy to observe that T_c is determined by non-axisymmetric mode $m = 1$ within $510 \leqslant Q \leqslant 6080$ and by axisymmetric oscillatory mode when Q is above 6080. The ratios for $m = 2$, 3, and 4 increase rapidly with Q as $Q > 670$. Figure 13(b) shows

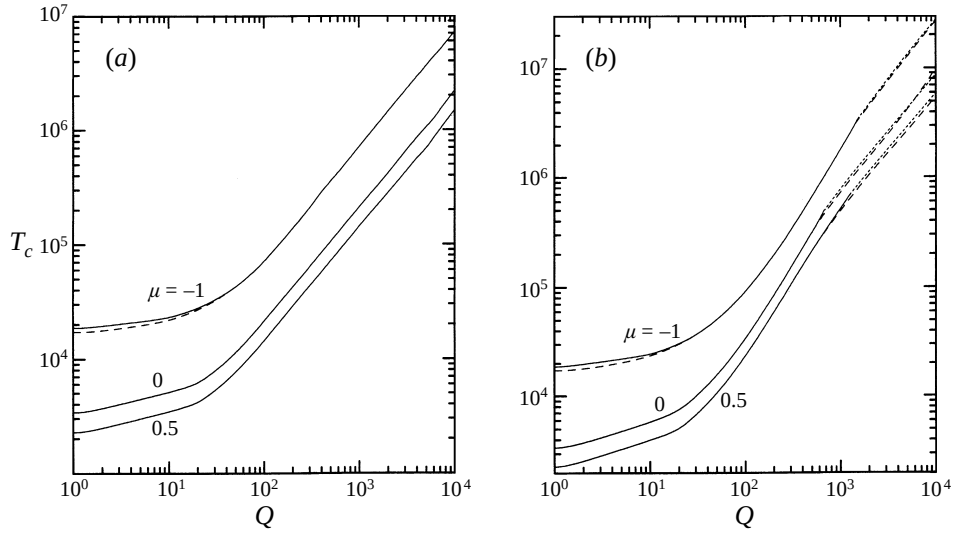

FIGURE 14. The variation of T_c with Q for assigned values of μ; ——, axisymmetric stationary mode; -----, axisymmetric oscillatory mode; – – –, non-axisymmetric mode (*a*) non-conducting walls, (*b*) conducting walls.

the results for $\mu = 0.5$. In order to distinguish the curves more clearly, solid and dashed curves are used alternately for each mode. We observe that non-axisymmetric disturbances prevail in a wide range of Q. This figure interprets the results obviously that T_c is determined by non-axisymmetric disturbances with $m = 1$, 2, and 1 corresponding to the ranges $550 \leqslant Q \leqslant 600$, $610 \leqslant Q \leqslant 2060$ and $Q > 2060$, respectively. We can predict that the critical disturbance will be the axisymmetric oscillatory mode at higher values of Q because the ratio for the curve $m = 1$ increases gradually with increasing Q. We also note that the azimuthal wavenumber m of the critical disturbance appears to increase with μ from the indication of figure 13. Indeed, we find the non-axisymmetric mode with higher azimuthal wavenumber may become critical as $\mu > 0.5$. It has been proved by Chang & Sartory (1967) analytically that axisymmetric oscillatory modes do not exist for corotating conducting walls at the special case $\mu = +1$. This indicates the upper boundary of the shaded area in figure 7 should tend to infinity as μ approaches $+1$.

In figure 14, the variation of the critical Taylor number T_c with Q for three assigned typical values of μ is shown for non-conducting and conducting walls, respectively, and the variation of T_c with μ for several selected high values of Q is also shown in figure 5(*a*) and 6(*a*). In general, T_c is still a monotonic increasing function of Q at high Hartmann number for all the μ considered. Of interest is the differences in the critical speed of the inner cylinder for axisymmetric and non-axisymmetric disturbances at different values of μ. For instance, as $\mu = 0$ and $Q = 1000$ for conducting walls, the corresponding critical values of T_c occur for $T_c^1 = 719872$ and $T_c^0 = 772491$. We have $(R_c^0 - R_c^1)/R_c^0 \sim 0.035$, which is more significant than the case we discussed at low Hartmann number, but is still a small percentage change. Thus, it may be difficult to distinguish the onset of instability modes by measuring the critical speed alone. In the related experiments of this flow, the onset of instability is detected by a change in the effective viscosity inferred from torque measurements. Roberts (1964) has mentioned that the change in torque will be a second-order effect for non-axisymmetric modes, thus, the evidence of the onset of instability will not be as dramatic as for the

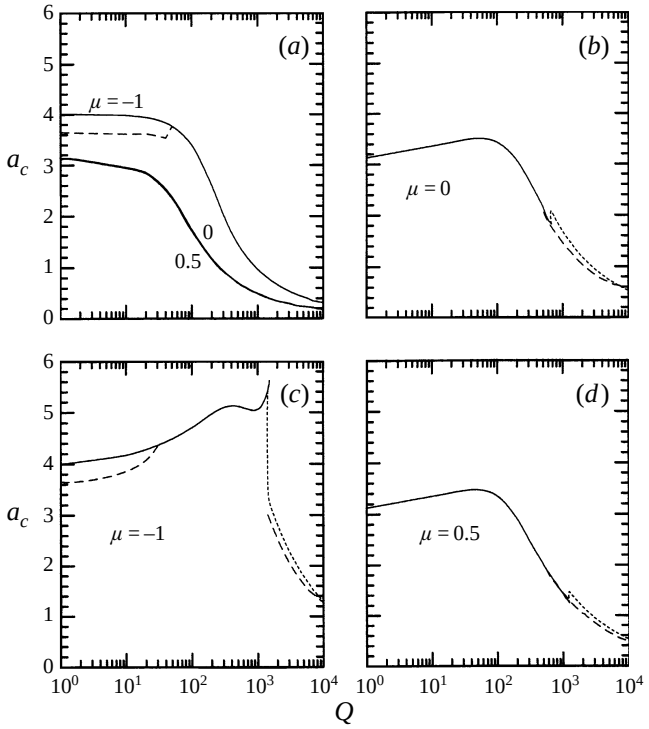

FIGURE 15. The variation of a_c with Q for assigned values of μ; (*a*) non-conducting walls; (*b–d*) conducting walls; ——, axisymmetric stationary mode; ----, axisymmetric oscillatory mode; – – –, non-axisymmetric mode.

axisymmetric mode. Furthermore, the experimental works of Donnelly & Caldwell (1964) reveal that the effective viscosity shows a slow systematic increase with Ω_1 before a sharp sudden change occurs as Q is large enough. They suggested that there may be a relatively weak instability before the onset of axisymmetric disturbance and the lowest mode of instability would be a non-axisymmetric one beyond a certain magnetic field. The onset was clearly defined only over a limited range of magnetic field strength in their experiments and the results indicate that the differences between the critical angular velocity of the inner cylinder for axisymmetric and non-axisymmetric disturbances should be significant. However, we note that the stainless-steel cylinders they used are not ideal electrical conducting walls, indicated by the results of Donnelly & Ozima (1962), and the variation of effective viscosity is considered to be affected by mercury and surface contamination, misalignment and eccentricity of the cylinders, as well as end effects. They mentioned that the accuracy falls off at low speeds owing to the decrease in torque, and the experiments were carried out with the expectation that the results would be qualitatively correct. However, their work indeed gave an important indication that the non-axisymmetric instability mode should be considered for the type of flow under study. It would be helpful to have more precise experimental works in order to determine the points of onset of the non-axisymmetric modes.

The variation of a_c with Q for assigned values of μ is shown in figure 15, and the variation of a_c with μ for several assigned high values of Q is also shown in figures 5(*b*) and 6(*b*). For non-conducting walls, a_c is generally a monotonic decreasing function of Q at high Hartmann number for all the μ considered, as shown in figure 5(*b*) and for three typical cases in figure 15(*a*). The discontinuities in slope of the curve for the non-

axisymmetric mode in figure 15(*a*) near $Q = 50$ are associated with switches between different modes. Both of the curves for $\mu = 0$ and 0.5 are almost coincident because for a given value of Q, a_c will tend to be a constant as $\mu \geqslant 0$, as shown in figure 5(*b*). For conducting walls, the variation of a_c with Q is more complex. Figure 15(*b*) illustrates the result for $\mu = 0$. Note that the variation of a_c is described by the gradual shift of the lowest branch of the neutral curves in the (T, a)-plane. In other words, a_c is determined by the gradual shift of the lower branch for axisymmetric stationary modes as $0 \leqslant Q < 510$ (see figure 8), a_c increases at first, reaches a maximum, then decreases with Q. Within $510 \leqslant Q \leqslant 6080$, a_c is described by the gradual shift of the neutral curve for the non-axisymmetric mode $m = 1$ to the left-hand side in the (T, a)-plane, so a_c decreases with Q. As $Q > 6080$, a_c is determined by the gradual shift of the neutral curve for axisymmetric oscillatory mode to the left-hand side in the (T, a)-plane, a_c still decreases with Q. We also find that when axisymmetric oscillatory mode becomes more critical, the corresponding value of a_c will be less than that of non-axisymmetric mode $m = 1$. Note that there is a sudden jump of a_c for axisymmetric disturbance near $Q = 670$ corresponding to the shift of the critical neutral curve from the left stationary loop to the right oscillatory curve in (T, a)-plane as we have mentioned. Similar discussion can be made for $\mu = -1$ and 0.5. For $\mu = -1$ as shown in figure 15(*c*), the jump of a_c associated with switches between different modes is not apparent near $Q = 30$ compared to non-conducting walls in figure 15(*a*) near $Q = 50$. However, at higher values of Q, a_c experiences a dramatic jump at $Q = 1430$ from axisymmetric stationary mode to non-axisymmetric mode $m = 1$ and decreases gradually with Q since a_c is determined by the gradual shift of the neutral curve for $m = 1$ to the left as $Q \geqslant 1430$ which is indicated by figure 10(*b*, *c*). There is also a finite jump of a_c for axisymmetric disturbance at $Q = 1520$ since the neutral curve of the oscillatory modes will dip lower than that of the stationary modes as $Q \geqslant 1520$ and shift to the left gradually with increasing Q. For $\mu = 0.5$, Chang & Sartory (1967) have given the results for the variation of a_c with Q by considering the normal modes of axisymmetric stationary disturbances only and found that a_c undergoes a series of discontinuities as Q increases. Instead of discussing the complex transition of the axisymmetric stationary normal modes with Q, we present here the results of the lowest branch of the neutral curves for axisymmetric and non-axisymmetric disturbances only. As shown in figure 15(*d*) for $\mu = 0.5$, the variation of a_c with Q is similar to the case $\mu = 0$. There is no occurrence of jump of a_c at $Q = 550$ as indicated in figure 11(*a*), and a_c is determined by the gradual shift of the neutral curve for non-axisymmetric mode to the left in the (T, a)-plane with increasing Q. The jump of a_c that occurs for axisymmetric disturbances at $Q = 1250$ is also due to the shift of the critical neutral curve from the left-hand stationary loop to the right-hand oscillatory curve, as shown in figure 11(*c*). In figure 6(*b*), the discontinuity of the curve for $Q = 1000$ between $-0.7 < \mu < -0.6$ is also due to the shift of the critical disturbance from the axisymmetric stationary mode to the non-axisymmetric mode. We use a dashed line to connect the discontinuity of a_c and note that the critical axisymmetric disturbance is the oscillatory mode at $\mu = -0.6$ with almost the same a_c as the non-axisymmetric mode. In general, a_c decreases at sufficiently high Hartmann number with increasing Q for all the μ considered and the onset mode is always accompanied by a least critical axial wavenumber.

It is also worth noting the frequency of the critical mode for axisymmetric oscillatory and non-axisymmetric disturbances. The non-axisymmetric modes are always oscillatory. The frequency, σ_i, occurs in positive–negative pairs for axisymmetric oscillatory modes, but not for non-axisymmetric modes. Figure 16 shows the variation

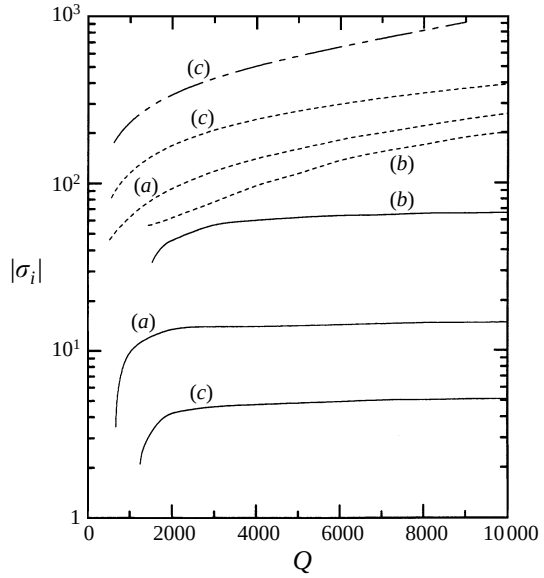

FIGURE 16. Variation of the frequency with Q. ——, $m = 0$; ----, $m = 1$; ————, $m = 2$, (a) $\mu = 0$, (b) -1, (c) 0.5.

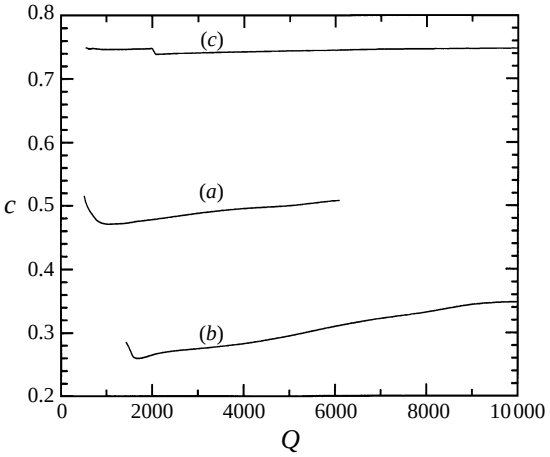

FIGURE 17. Variation of the critical angular velocity c with Q; (a) $\mu = 0$, (b) -1, (c) 0.5.

of the frequency $|\sigma_i|$ with Q for conducting walls, and several assigned values of μ and m where $m = 0$ represents the axisymmetric oscillatory mode. The curves for $\mu = 0$ and -1 as $m = 0$ have been given by Chang & Sartory (1967). They noted that at the onset of axisymmetric oscillatory instabilities, the frequency $|\sigma_i|$ increases rapidly with Q, then levels off and becomes almost constant shortly after the transition. Here, we consider further including the additional case $\mu = 0.5$ and the corresponding critical non-axisymmetric modes. For a fixed sufficiently high value of Q, it is found that the frequency $|\sigma_i|$ of axisymmetric oscillatory mode is generally a monotonic decreasing function of μ and gradually approaches zero as $\mu \to 1$. On the other hand, the frequency $-\sigma_i$ of the non-axisymmetric mode increases with Q after the onset of instabilities is dominated by the non-axisymmetric mode, and increases with increasing μ for fixed

values of Q and m as shown in figure 16 for $m = 1$, and increases with higher value of the azimuthal wavenumber m for given values of μ and Q.

Figure 17 illustrates the variation of the critical angular velocity c in units of Ω_1 of the azimuthal travelling wave with Q for conducting walls with three typical values of μ. It is to be noted that the value of c generally decreases at first, then increases slightly with Q. The discontinuities in slope for the curve $\mu = 0.5$ are also due to the shift in critical instability modes. For a given sufficiently high Hartmann number, the critical angular velocity c is a monotonic increasing function of μ.

4. Conclusions

We have conducted a complete analysis for the onset of secondary motion of hydromagnetic dissipative Couette flow in a small-gap spacing between two infinitely long rotating cylinders with a uniform magnetic field applied in the axial direction. The results of the present study show that this flow exhibits distinct stability characteristics depending on the conductivity of the cylinders. For non-conducting walls, the onset of instability is the non-axisymmetric mode when μ is sufficiently negative and the corresponding range of Q is limited. When μ is less than the critical value -0.78, the critical azimuthal wavenumber m decreases with increasing Q for fixed μ. The variation is, of course, not continuous since the azimuthal wavenumber takes on only integer values. The critical disturbances are always axisymmetric stationary modes excluding the limited domain where non-axisymmetric modes prevail. For conducting walls, the stability characteristics are alike with non-conducting walls at low Hartmann number but not at high values of Q. It is found that non-axisymmetric instability modes become more critical again when Q is above some critical value which depends on μ and prevail in a wide range of Q. At higher Hartmann number, the onset of instability would be dominated by axisymmetric oscillatory modes. We identify the instabiity mode in the plane (μ, Q) which covers $-1 \leqslant \mu < 1$ and $0 \leqslant Q \leqslant 10000$, and show the domain where each instability mode prevails. Results for three typical cases, including $\mu = 0, -1$, and 0.5, are shown in detail. The present calculations reveal that non-axisymmetric instability modes play an important role once the magnetic field effect becomes significant for conducting walls. However, additional experimental information on the subject is clearly required.

The financial support for this work from the National Science Council of Taiwan through Grant no. NSC 85-2212-E-006-070 and the aid of computer resources from the National Center for High-Performance Computing are gratefully acknowledged. The authors also wish to thank the reviewers for their detailed and helpful comments which enhanced the clarity of the paper.

REFERENCES

Andereck, C. D., Lin, S. S. & Swinney, H. L. 1986 *J. Fluid Mech.* **164**, 155.

Chandrasekhar, S. 1953 *Proc. R. Soc. Lond.* A **216**, 293.

Chandrasekhar, S. 1954 *Mathematica* **1**, 5.

Chandrasekhar, S. 1961 *Hydrodynamic and Hydromagnetic Stability*. Clarendon.

Chang, T. S. & Sartory, W. K. 1967 *Proc. R. Soc. Lond.* A **301**, 451.

Chen, F. & Chang, M. H. 1992 *J. Fluid. Mech.* **243**, 443.

Chossat, P. & Iooss, G. 1994 *The Couette–Taylor Problem*. Springer.

Coles, D. 1965 *J. Fluid. Mech.* **21**, 385.

Davey, A., DiPrima, R. C. & Stuart, J. T. 1968 *J. Fluid Mech.* **31**, 17.
DiPrima, R. C. 1955 *Q. Appl. Maths.* **13**, 55.
DiPrima, R. C. 1960 *Q. Appl. Maths.* **18**, 275.
Donnelly, R. J. & Caldwell, D. R. 1964 *J. Fluid Mech.* **19**, 257.
Donnelly, R. J. & Ozima, M. 1962 *Proc. R. Soc. Lond.* A **266**, 272.
Harris, D. L. & Reid, W. H. 1964 *J. Fluid Mech.* **20**, 95.
Hassard, B. D., Chang, T. S. & Ludford, G. S. S. 1972 *Proc. R. Soc. Lond.* A **327**, 269.
Krueger, E. R., Gross, A. & DiPrima, R. C. 1966 *J. Fluid Mech.* **24**, 521.
Kurzweg, U. 1963 *J. Fluid Mech.* **17**, 52.
Nissan, A. H., Nardacci, J. L. & Ho, C. Y. 1963 *AIChEJ.* **9**, 620.
Roberts, P. H. 1964 *Proc. Camb. Phil. Soc.* **60**, 635.
Sparrow, E. M., Munro, W. D. & Jonsson, V. K. 1964 *J. Fluid Mech.* **20**, 35.
Tabeling, P. 1981 *J. Fluid Mech.* **112**, 329.
Takhar, H. S., Ali, M. A. & Soundalgekar, V. M. 1989 *Appl. Sci. Res.* **46**, 1.
Taylor, G. I. 1923 *Phil. Trans. R. Soc. Lond.* A **223**, 289.
Weinstein, M. 1977*a* *Proc. R. Soc. Lond.* A **354**, 441.
Weinstein, M. 1977*b* *Proc. R. Soc. Lond.* A **354**, 459.